

PETRA qMRA: Towards Zero-Flow Dephasing Intracranial Non-Contrast MR Angiography

Yutaka Natsuaki¹, Xiaoming Bi¹, David M Grodzki², Aurelien F Stalder², and Gerhard Laub¹
¹Siemens Healthcare, Los Angeles, CA, United States, ²Siemens Healthcare, Erlangen, Germany

Target Audience: Clinicians and researchers with interest in an intracranial non-contrast MR Angiography without flow dephasing artifacts.

Purpose: The 3D time-of-flight sequence with MOTSA (3D TOF) [1] has been considered as a gold-standard for an intracranial non-contrast MR Angiography (MRA). The 3D TOF, however, has well known flow dephasing artifacts in lumen, in particular in the tortuous carotid arteries. Recently, ultra-short TE (UTE) sequences have evolved into the zero-TE (ZTE) sequences (e.g. PETRA [2]), and their inherent zero flow dephasing property is highly desirable in the aforementioned MRA applications. By acquiring two ZTE data sets of different lumen contrasts and by subtracting these, zero-flow dephasing MRA can be achieved (e.g. PETRA qMRA[3]). The current work demonstrates a possibility of utilizing the optimized PETRA qMRA as a viable alternative to the current gold-standard 3D TOF.

Methods: The PETRA sequence consists of 2 distinctive parts: the ZTE 3D radial projection part (Fig.1a) and the point-wise Cartesian acquisition part (Fig.1b). Without a specialized hardware, Tx/Rx switching time (T_{HW} in Fig.1a) in the conventional MR scanners cannot perform fast enough for ZTE, and every radial projection creates a gap in the middle of the k-space. The shortcomings are then compensated by the Cartesian point-wise acquisition, filling in the spherical gap, one Cartesian k-space point at time (Fig.1c).

For the PETRA qMRA, two data sets (the labeled and the control) are acquired. The labeled data set applies the slice-selective saturation pulse at the upstream of the carotid artery, effectively darkening the arterial inflow. The subsequent control data features the same saturation pulse, only prescribed outside of the imaging volume for the MT effects while not interfering with the imaging volume. Two data sets are then subtracted to generate desired Arterial MRA with back ground tissue and venous flow suppressed.

As with any subtraction-based MRA techniques, the two data sets need to match closely; the intervoxel motion and the background tissue contrast are carefully considered. The center of the k-space, which is embedded in the Cartesian part, is more sensitive to subject motion, and two consecutive acquisitions of the same parts order (e.g. radial part first in Fig.2) are less desirable. Instead, we propose to acquire the Cartesian part first for the second data set, thus minimizing the time distance of the Cartesian parts. Moreover, the background contrast of the two data sets is matched by applying steady state preparation at the beginning of each acquisition (Fig.2).

The sequence prototype was implemented on 3.0T scanners (Magnetom Skyra and Prisma, Siemens Healthcare, Erlangen, Germany). The technique was validated with healthy volunteers (n=5) under a local IRB approved protocol. PETRA qMRA data was acquired with the following protocol: FOV 220mm³, 65000 radial spokes; isotropic 0.86mm³; flip angle = 3°; TR/TE 3.18/0.07msec; BW 1860 Hz/pixel; slice selective Saturation pulse applied once per 25 TRs; total scan time 2 x 4:07min. For the comparison purpose, 3D TOF with a typical clinical protocol (FOV 220mm, 3 axial slabs 25% overlapped; acquisition voxel size = 0.48 x 0.48 x 0.65 mm³ (slice interpolated to 0.4mm); flip angle = 18°; TR/TE = 23.0/3.8 msec; BW 248 Hz/pixel; GRAPPA acceleration 2; slice Partial Fourier 7/8; total scan time 5:20 min) was acquired on the each volunteer. The resulting MRA data sets were compared for overall image quality, delineation of vessel details, and presence/absence of artifacts.

Results: All volunteer scans and reconstructions were performed successfully. Despite having a slightly worse resolution with PETRA qMRA, the overall image quality and delineation of vessel details are closely matched with that of 3D TOF. In all of the volunteer cases, 3D TOF has demonstrated flow dephasing artifacts while the PETRA qMRA has no such artifacts shown (representative case shown in Fig.3).

Discussion: PETRA's ZTE advantage goes beyond just the flow dephasing. Fat enhancement effect observed in the previous UTE sequences is no longer apparent. Air-tissue interface artifacts are also reduced. Despite the fact that the slice selective saturation pulse adds acoustic noise to otherwise extremely quiet PETRA (65dB), PETRA qMRA (74dB) is still significantly quieter than any other MRA sequences such as 3D TOF (100dB). While there exist more sophisticated labeling and background suppression techniques (e.g. pcASL, [4]), these IR-based labeling schemes require more scan time (TI and recovery time) and are thus not practical with our current non-accelerated PETRA qMRA.

Conclusion: PETRA qMRA shows promising results without flow dephasing artifacts. Further clinical testing for intracranial MRA and R&D efforts are granted.

References: [1] Parker DL et al. MRM 17:434-451(1991) [2] Grodzki DM, et al. MRM 67:510-518 (2012) [3] Grodzki DM et al. Proc. MRA Club (2014) [4] Wang JJ et al. JMIR 39:1320-1326 (2014)

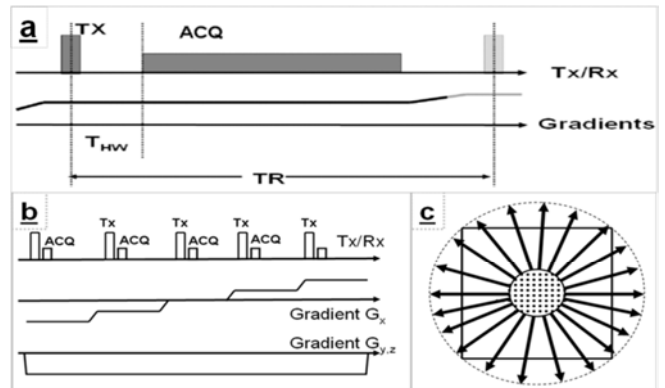


Fig.1: Schematic diagram of the PETRA sequence. The sequence consists of (a) the zero-TE 3D radial projection and (b) the point-wise Cartesian acquisition. Corresponding k-space trajectory is depicted in (c).

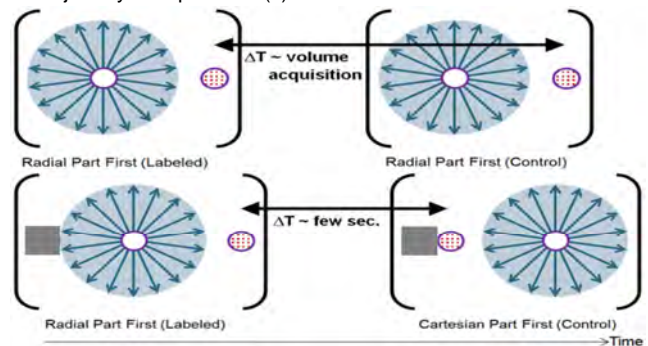


Fig.2: Schematic diagram of the conventional PETRA qMRA with repeated Radial part First (upper row) and the optimized PETRA qMRA (bottom row). In addition to the reversed order, steady state preparation (square) is applied.

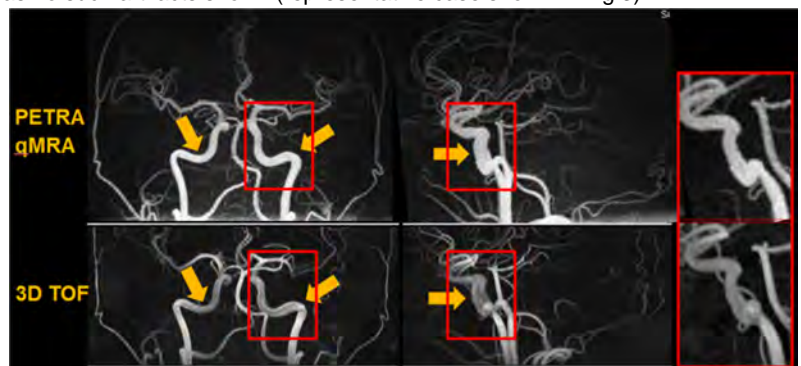


Fig.3: Representative coronal, sagittal and zoomed sagittal left carotid artery sub volume MIP comparisons of the PETRA qMRA vs. the conventional 3D TOF. As indicated by the arrows, TOF shows flow dephasing artifacts, while PETRA qMRA has shown no signs of dephasing.